

# 1 Thermodynamic Aspects

## 1.1 Combustion System

Combustion system, S, is a confined field of a compressible fluid where the exothermic process of combustion takes place, subject to conditions imposed at its boundary. Presented here are global properties of such a system.

The composition of a combustion system is specified by mass fractions of its initial components,  $Y_K$ , where  $K = F, A$  and  $B$ , for, respectively, fuel, air and the non-reacting portion of the fluid, like the recirculated exhaust, or residual gas. The mass fraction of reactants,  $Y_R = Y_F + Y_A$ , a mixture of fuel and air, is equal to that of the reaction products,  $Y_P$ .

The composition of a combustible mixture is expressed by the air/fuel ratio,  $\sigma_K \equiv (Y_A / Y_F)_K$ , ( $K = R, S$ ). For the reactants,  $\sigma_R$  is identified usually with the measured flow rates of air and fuel, whereas for the system,  $\sigma_S$  is deduced from the exhaust gas analysis. The values of these ratios are expressed conventionally in terms of the air-equivalence ratio with respect to the stoichiometric proportion, referred to by subscript "st",  $\lambda_K \equiv \sigma_K / \sigma_{st}$ , reciprocal of the fuel-equivalence ratio,  $\phi_K$ .

Thus,

$$Y_K \equiv (1 + \sigma_K) Y_F \equiv (1 + \sigma_{st} \lambda_K) Y_F \quad (1.1)$$

whence, for the same mass fraction of fuel,  $Y_F$ ,

$$\frac{Y_F}{Y_K} = \frac{1}{1 + \sigma_K} = \frac{1}{1 + \sigma_{st} \lambda_K} \quad (1.2)$$

A phase diagram of the mass fraction of system components is displayed in Fig.1.1 with respect to the mass fraction of products,  $y_P$ , i.e. the substance produced by oxidation of fuel and their mixing with the non-reacted portion of the cylinder charge. The variable mass fractions are denoted in it by small letters and the constants defining the system by capital letters.

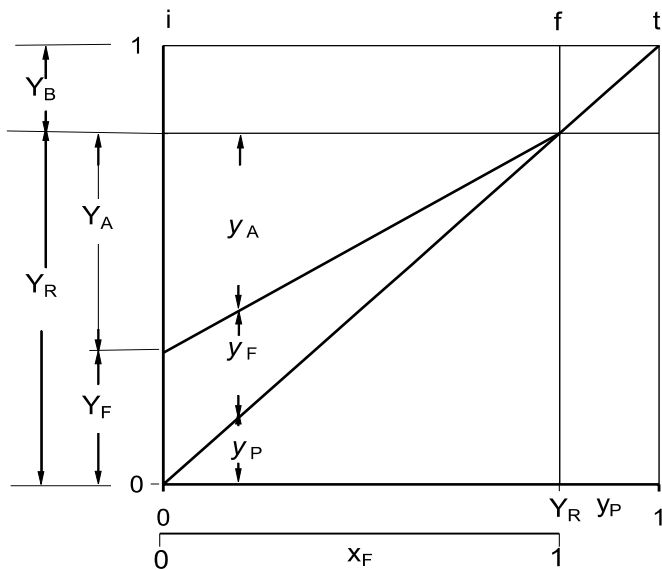


**Fig. 1.1.** Phase diagram of component mass fractions with respect to mass fraction of products

As displayed by this figure, in the course of combustion the mass fractions of components,  $y_K$  ( $K = F, A$ ), are linear functions of the mass fraction of end products,  $y_P$ , namely

$$y_K = \frac{Y_K}{Y_R}(Y_R - y_P) \quad (1.3)$$

while the latter is expressed in terms of the mass fraction of fuel,  $x_F$ , as

$$y_P = Y_R x_F \quad (1.4)$$

For a system constrained by the walls of its enclosure, like a cylinder in a piston engine, the sole purpose of combustion is to generate pressure. With a measured pressure profile, the objective of its thermodynamic

analysis is the solution of an inverse problem: the deduction on this basis of data on the evolution of the thermodynamic state parameters of the system components, as well as of the mass fraction of combustion products – a quantity proportional, according to (1.4), to that of fuel.

Mass fractions of fuel,  $x_F$ , and of products,  $y_P$ , consist of the effective parts,  $x_E$  and  $y_E$ , formed to produce the measured pressure profile, and of the ineffective parts,  $x_I$  and  $y_I$ , expended by energy loss due primarily to heat transfer to the walls of the enclosure, i.e.  $x_F = x_E + x_I$  and  $y_P = y_E + y_I$ .

Their profiles are displayed by Fig. 1.2 in terms of the normalized time,  $\tau \equiv (t - t_i)/T$ , where, with  $t_f = t_b$ ,  $T = t_f - t_i$  is the lifetime of the exothermic process that shifts the process of expansion away from that of compression to form the work cycle. As demonstrated in Chapter 3, the initial state, **i**, at  $\tau=0$ , is a fundamental, sharp, saddle type, singularity of combustion, while the final state, **f**, occurring at the same time as the terminal state, **t**, is at  $\tau=1$  – the end of the exothermic process identified above – where the effective parts,  $x_E$  and  $y_E$ , are at their maxima forming a smooth, nodal type, singularity.

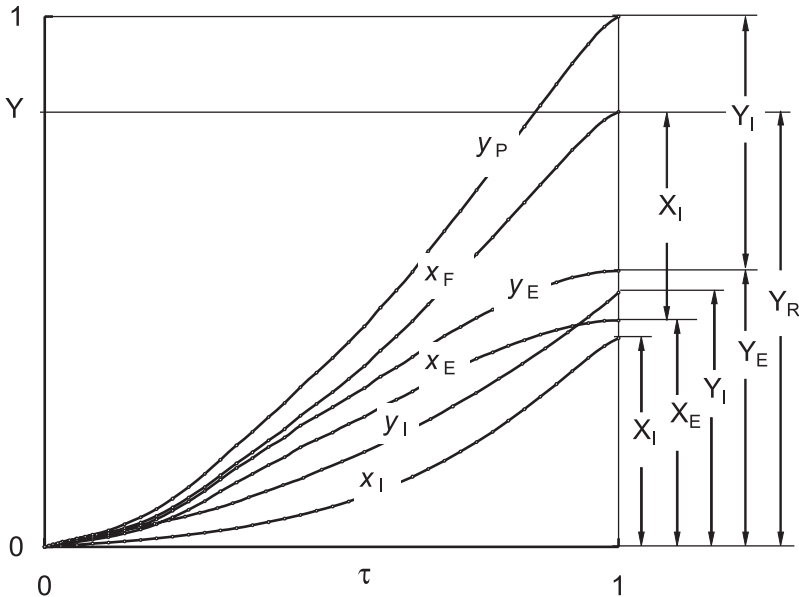


**Fig. 1.2.** Profiles of effective and ineffective mass fractions of fuel and products

Global properties of a combustion system are established by *pressure diagnostics* – a procedure for solution of an inverse problem based on measured pressure,  $p$ , and given mass averaged specific volume,  $v$ . The procedure of pressure diagnostics consists of two perspectives:

1. *Dynamic Properties* manifested by the physical space of the work cycle. Their parameters are derived directly from data of the measured pressure profiles,  $p(t)$ , and the corresponding volume profiles,  $v(t)$ , obtained from the crank-angle mechanism of the engine. Besides coordinates of the work cycle,  $p(v)$ , they provide data for the profile of the *dynamic potential*,  $w(t) \equiv p(t)v(t)$ , exposed in Section 1.2.1, and their expressions in terms of analytic functions, described in Section 1.2.2.

2. *Thermodynamic Properties* manifested by the thermodynamic phase space delineating the three component processes of the: compression, the exothermic process referred to as the *dynamic stage*, and expansion. The fundamental reference coordinate of this space is the dynamic potential,  $w(t)$ . The trajectories of the processes carried out by the system in the course of the work cycle are delineated on the state diagram,  $e(w)$ , where  $e$  is the internal energy of the working substance. Obtained on this basis are profiles of the temperature,  $T(t)$ , as well as of the effective mass fractions of products,  $y_p(t)$ , and, hence, of fuel expended to create pressure,  $x_F(t)$ .

## 1.2 Dynamic Properties

The analysis of the dynamic properties yields analytic expressions for the exothermic process (popularly referred to as ‘heat release’) of combustion. It takes place in the course of, what is here referred to, the dynamic stage. Its life time is identified by the bounds: the rank angle of the initial state, **i**, and that of the final state, **f**. State **i** is an essential singularity of combustion, a saddle point representing the state where the specific volume of the products,  $v_i = V_i / M_i = 0/0$  (!) – the *raison d’être* of what is known in combustion literature as the “cold-boundary difficulty,” occurring in laminar flames (Williams 1985). Since nature abhors corners, it is bypassed by experimental data and, hence, state **i** is not identifiable by a data point.

State **f**, is at a singular point of maximum in the evolution of the combustion system, where its support by the deposition of exothermic energy is at equilibrium with the endothermic loss of energy incurred by heat transfer to the walls.

### 1.2.1 Dynamic Potential

The dynamic potential

$$w \equiv pv \equiv \frac{p}{\rho} \equiv h - e \quad (1.5)$$

is of particular significance to pressure diagnostics by furnishing an essential link between the dynamic Properties, where it is evaluated as a dependent variable, and the thermodynamic Properties for which it provides the fundamental thermodynamic reference parameter. The temperature is delegated thereby to the position of a dependent variable. Its magnitude can be readily determined from the equation of state for given values of  $p$  and  $w$ , or  $v$ , of the substance.

By expressing the specific volume in a non-dimensional normalized form,  $w$  is measured in units of pressure. Its value is popularly called flow work - a term demeaning its cardinal nature, as pointed out by Kestin 1966 (Sections 4.1 and 4.2). The significance of the dynamic potential is emphasized by most equations of state. For example, consider the following equations.

Van der Waals: 
$$w = \frac{R}{M} T \frac{v}{v-b} - \frac{a}{v}$$

Dietrich: 
$$w = \frac{R}{M} T \frac{v}{v-b} e^{-a/vRT}$$

Beattie-Bridgeman: 
$$w = \frac{R}{M} T + \frac{\beta}{v} + \frac{\gamma}{v^2} + \frac{\delta}{v^3}$$

BKW<sup>1</sup>: 
$$w = \frac{R_u}{M} T \left[ 1 + x e^{\beta x} \right] \quad x = \frac{k}{v(T + \vartheta)^\kappa}$$

JWL<sup>2</sup>: 
$$w = A \left[ 1 - \frac{v}{c_{v1} v_c} \right] v e^{-R_1 v/v_c} + B \left[ 1 - \frac{v}{c_{v2} v_c} \right] v e^{-R_2 v/v_c} + \frac{R}{c_v} u$$

Virial Equation of State: 
$$w = A(\Theta) + B(\Theta)p + C(\Theta)p^2 + \dots$$

In the latter,  $\Theta \equiv \frac{w_m}{\mathcal{R}}$ , where subscript  $m$  implies that the dynamic potential,  $w$ , is expressed per mole of the substance, while  $\mathcal{R}$  is the universal gas constant.

<sup>1</sup> Becker-Kistiakowski-Wilson

<sup>2</sup> Jones-Wilkins-Lee

It is, in fact, for this reason that an equation of state for a system in equilibrium can be determined experimentally without measuring the temperature – a procedure providing the measure for the absolute temperature scale (vid. e.g. Kestin 1966-68).

### 1.2.2 Data

The procedure for establishment of the dynamic Properties is illustrated here by the specific example of a HCCI (Homogeneous Charge Compression Ignition) engine – a system that today is at the crest of popular research on novel piston engines. The data of the engine adopted for the present purpose are provided by Table 1.1. The operating conditions of its dynamometer test are listed in Table 1.2.

**Table 1.1.** HCCI engine data

Bore (cm)	7.95
Stroke (cm)	9.56
Length of piston rod (cm)	14.4
Compression ratio	16.5
Intake valve closing, $\Theta_a$	205
$p_a$ (bar)	1.39
$T_a$ (K)	325
Exhaust valve opening $\Theta_z$	512

**Table 1.2.** Operating conditions

Speed	rpm	1200
Torque	Nm	75
Fuel (gasoline)	Octane No.	87
Stoichiometric air/fuel ratio	$v_{st}$ , mol/mol	12.305
	$\sigma_{st}$ , gm/gm	15.064
Air-equivalence ratio, $\lambda_S$ ,	-	2.2
Cylinder pressure at $\Theta_a$ , $p_a$ ,	atm	1.39
Gas temperature at $\Theta_a$ , $T_a$ ,	K	325

The air equivalence ratio cited in Table 1.2 was obtained from exhaust gas analysis and pertains therefore to the system, S, rather than the reactants, R.

Profiles of the dynamic parameters in terms of the crank angle,  $\Theta$ , provided by the dynamometer test data of the engine operating at constant speed, are presented in Figs. 1.3-1.6.

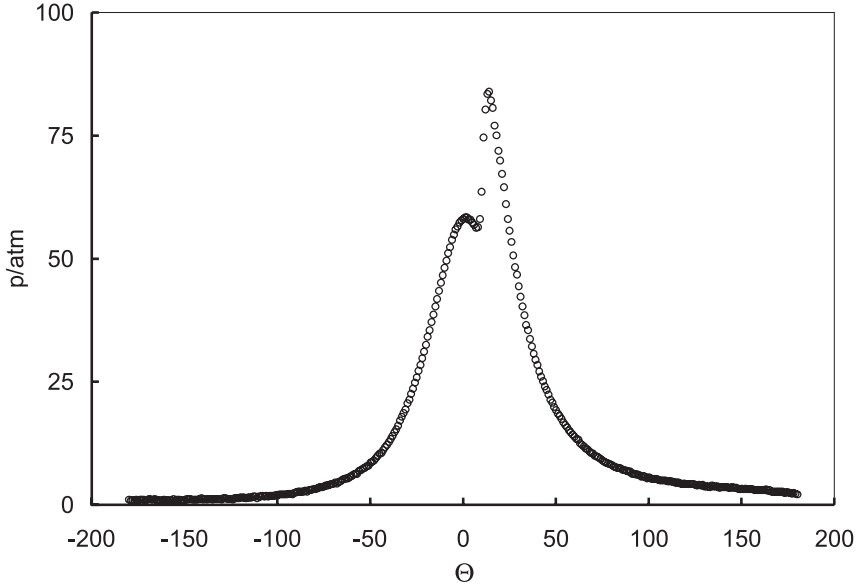


**Fig. 1.3.** Data of the pressure profile

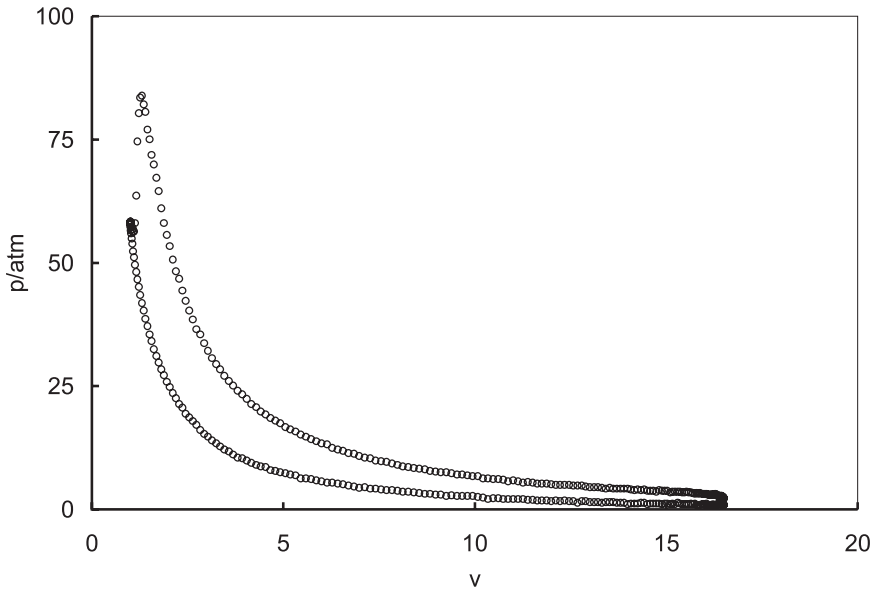


**Fig. 1.4.** Data of the work cycle in linear scales

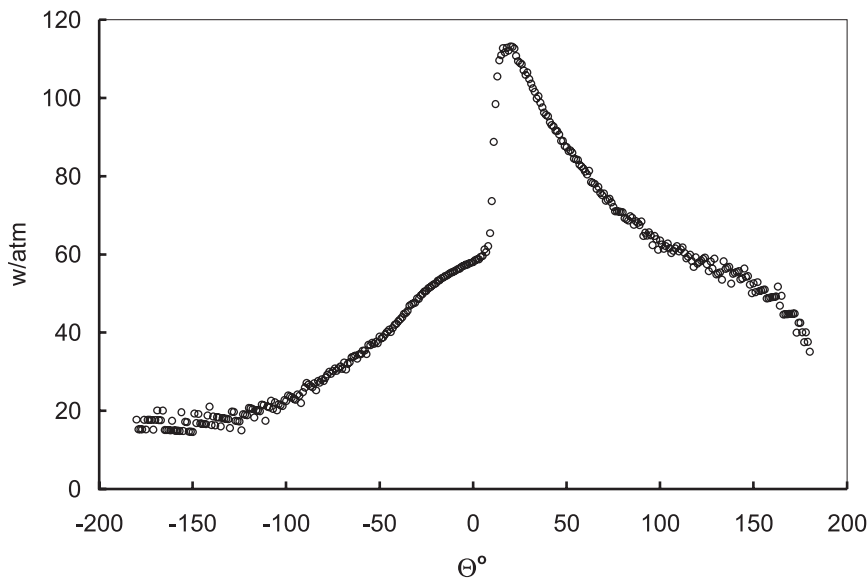


**Fig. 1.5.** Data of the dynamic potential

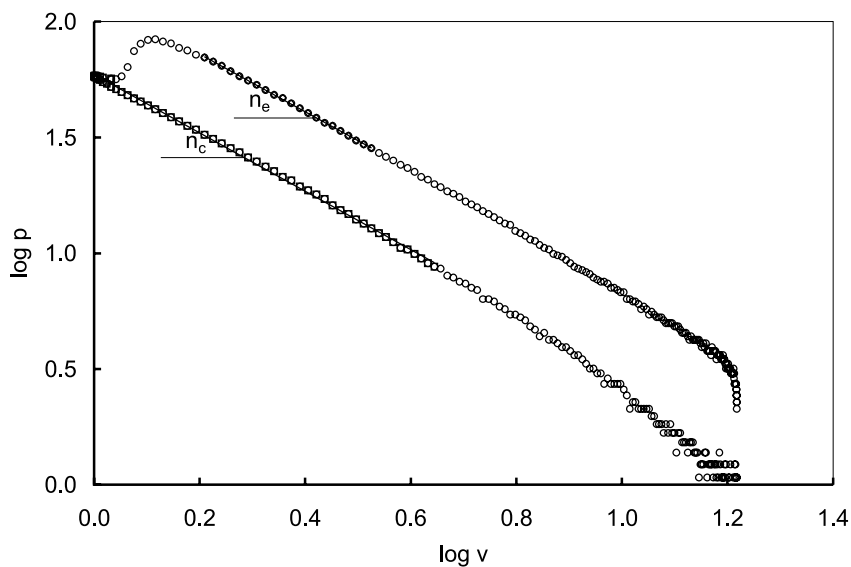


**Fig. 1.6.** Data of the work cycle in logarithmic scales

One should note that in pressure diagnostics  $v \equiv v_s / v_c$ ,  $c$  denoting clearance, and, since in dynamometer tests engines are operated at constant speed, the time,  $t$ , is expressed in terms of the crank angle,  $\Theta$ .



### 1.2.3 Functions

To provide a rational interpretation of the test data, they are expressed in terms of analytic functions. The key to this task is the polytropic function

$$\pi_k \equiv p v^{n_k} \quad (1.6)$$

where  $k = c, e, d$  for, respectively, the processes of compression, expansion, and the dynamic stage between them. In the first edition of this book and in Oppenheim 2004, the polytropic function was referred to by its generic name “polytropic pressure model”, because for an enclosure of constant volume  $n_k=0$ , so that  $\pi_k=p$ .

Upon selection of the scope of the data for analytic interpretation, bounded by point **b** at the start of the last sector of compression and point **c** at the end of the first sector of expansion, their processes are expressed by polytropes – functions for which  $n_c$  and  $n_e$ , as well as  $\pi_c$  and  $\pi_e$ , are constant. In Fig. 1.6, these polytropes are identified by straight-linear sectors between the postulated bounds, **b** and **i**- for compression and **f**+ and **c** for expansion, where the two exponents are identified by their slopes.

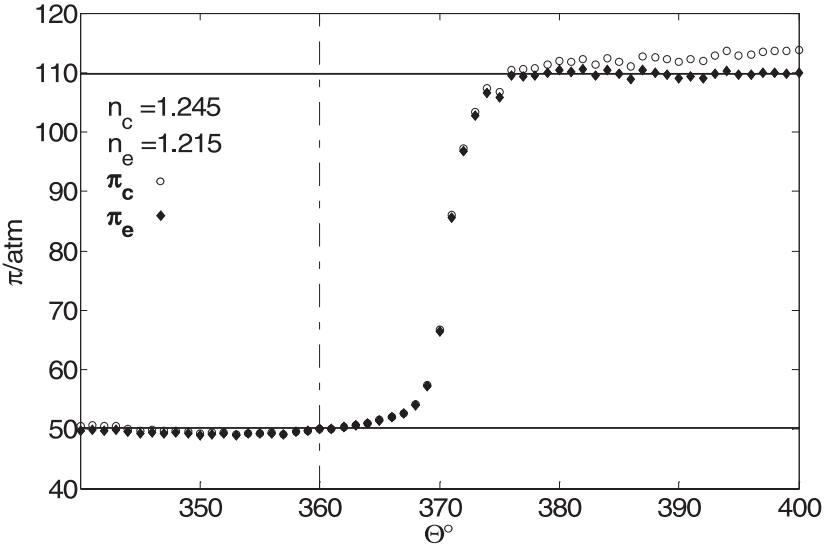


**Fig. 1.7.** Profiles of data for polytropic functions, evaluated with invariant indexes  $n_c$  (open points), and  $n_e$  (closed points)

Profiles of data expressed by polytropic functions of the HCCI engine, with  $n_c$  for compression and  $n_e$  for expansion, are portrayed by Fig. 1.7, where the two polytropes, extended over the width of the diagram, are displayed by horizontal lines.

The a priori unknown bounds of the analytic function for the dynamic stage,  $x_d$ , the initial point, **i**, and final point, **f**, must be located on these lines. To satisfy this requirement, the analytic function has to be established by iteration, with an, at least, partially variable exponent  $n_d$ .

The initial point is, therefore, first estimated to be ahead of the eventual position of **i**, at point **i**-, where the data of  $\pi_c$  start to rise above the horizontal polytrope for compression, and the final point postulated to be beyond the expected position of **f**, at point **f**+, where the data of  $\pi_e$  start to drop below the horizontal polytrope of expansion. The exponent of expansion,  $n_e$ , is retained below point **f** to some intermediate point, **n**, where the data of  $\pi_c$  and  $\pi_e$  are coincident. Up to that point, the polytropic function of the dynamic stage is expressed in terms of  $n_d = n_e$ . Below this point, it has to culminate at the initial point **i** on the extended polytrope of compression that, as brought out at the outset of Section 1.2, is a sharp singularity obviated by the data, for nature abhors corners.

For this purpose, the data of the dynamic stage are expressed in terms of the progress parameter for the polytropic function

$$x_k(\pi) = \frac{\pi - \pi_o}{\pi_k - \pi_o} \quad (k = n, f) \quad (o = i-, i) \quad (1.7)$$

in terms of which

$$n = n_c + (n_e - n_c)x_n(\pi) \quad (1.8)$$

Upon establishing in this manner the progress parameter,  $x(\pi)$ , made out of two sectors, one from **i**- to **n** according to (1.8), and the other from **n** to **f**+, with  $n = n_e$ , a unique analytic function for the dynamic stage is, obtained by regression of  $x(\pi)$ , between **i** and **f** to the life function introduced in Chapter 2 – a normalized exponential

$$x = \frac{e^{\zeta} - 1}{e^{\zeta_f} - 1} \quad (2.47)$$

whose exponent

$$\zeta = \frac{\alpha}{\chi + 1} [1 - (1 - \tau)^{\chi + 1}] \quad (2.48)$$

is a power function of the progress parameter for time that, for an engine operating at constant speed, is measured in terms of the crank angle,  $\Theta$ , i.e.

$$\tau \equiv \frac{\Theta - \Theta_i}{\Theta_f - \Theta_i} \quad (1.9)$$

For this purpose, the exact position of point **i** is established by iteration to minimize the standard deviation of regression, yielding the two life function parameters,  $\alpha$  and  $\chi$ .

As demonstrated in Chapter 2, the life function thus determined satisfies both conditions imposed by the singular boundaries of the dynamic stage, specified at the outset of Section 1.2.

Analytic interpretation of the profiles of the polytropic functions for the HCCI engine, are presented by Fig. 1.8, in comparison with data of Fig. 1.7.

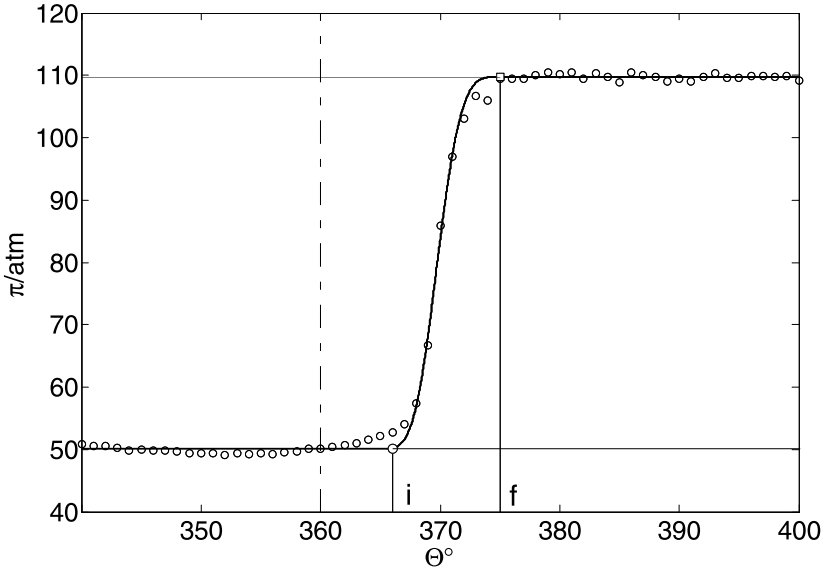


**Fig. 1.8.** Analytic interpretation of data for the last sector of compression, the dynamic stage, and the first sector of expansion of the HCCI engine

Values of all the parameters involved in this procedure for the HCCI engine are listed in Table 1.3, together with the crank angles of all the critical points for pressure diagnostics. The consecutively evaluated analytic interpretation of data for profiles of the dynamic potential, the work cycle, and pressure, are displayed, respectively, by Figs. 1.9, 1.10 and 1.11.

**Table 1.3.** Parameters of Dynamic Properties

Crank angle of point a	205°
Crank angle of point b	320°
Crank angle of point i	366°
Crank angle of point f	375°
Crank angle of point c	500°
Crank angle of point z	512°
Life function coefficient, $\alpha$	13.55
Life function exponent, $\chi$	2.19

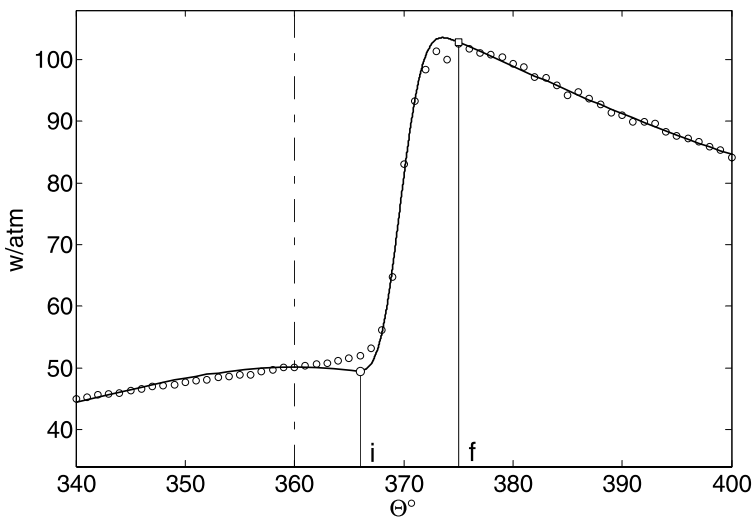


**Fig. 1.9.** Analytic interpretation of data for the dynamic potential of the HCCI engine

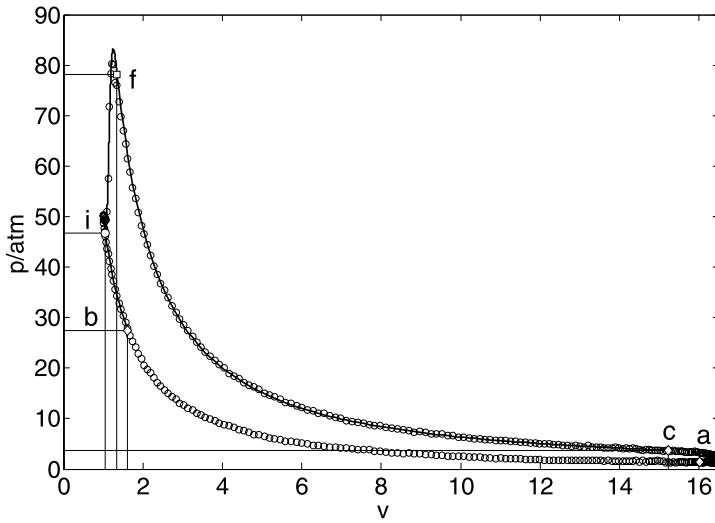


**Fig. 1.10.** Analytic interpretation of data for the work cycle of the HCCI engine

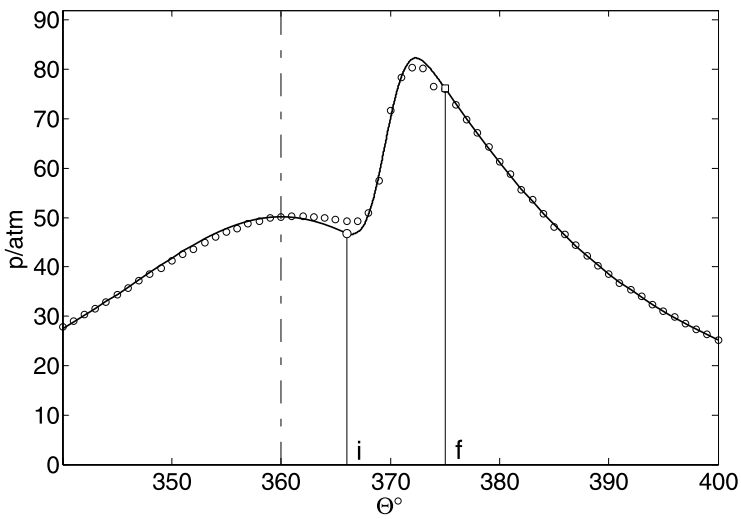


**Fig. 1.11.** Analytic interpretation of data for the pressure profile of the HCCI engine

## 1.3 Thermodynamic Properties

In accord with the zero-dimensional nature of dynamic properties, the variables of thermodynamic  $p$  are expressed in terms of time-dependent mass averaged thermodynamic parameters of state: the pressure,  $p_K(t)$ , the temperature,  $T_K(t)$ , the specific volume,  $v_K(t)$ , the internal energy,  $e_K(t)$ , and the dynamic potential,  $w_K(t)$ , where  $K = F, A, B, C, R$  and  $P$ , providing a link between the dynamic and thermodynamic properties. Moreover, since all the parameters of the dynamic properties are expressed in terms of analytic functions, the time coordinate can be expressed in terms of any of them, in particular pressure whose time profile provides the basis for their evaluation.

### 1.3.1 Thermodynamic State

The state of a constituent is identified by three parameters of its own equilibrium. The conventional equation of state, expressing a relationship between pressure,  $p$ , specific volume,  $v$ , and temperature,  $T$ , does not provide a comprehensive specification of state, because, to evaluate internal energy,  $e$ , specific heats are, moreover, required. If, however, internal energy is included among the parameters of state, then, according to the fundamental principle of the First Law provided by Gibbs (1875-1878) and formulated by Poincaré (1892) and Carathéodory (1909), the state of a constituent is thereby completely specified.

Accordingly, the thermodynamic state of a constituent is expressed by a point in a three-dimensional thermodynamic phase space whose coordinates are specific internal energy,  $e$ , specific dynamic potential,  $w$ , and pressure,  $p$ . If internal energy is expressed in molar (volumetric) basis, the fundamental role of a reference coordinate is played by the temperature,  $T$ , rather than  $w$ . However, since in system undergoing a chemical reaction mass is conserved rather than volume, the latter is for this purpose more appropriate.

The reactants,  $R$ , are considered as an air/fuel mixture at its local air-equivalence ratio,  $\lambda_R$ . The products,  $P$ , are specified by the molecular composition of the system at thermodynamic equilibrium. The states of both of them are established by appropriate algorithms. Their thermodynamic parameters are presented by Table 1.4 upon evaluation by means of STANJAN (Reynolds 1996), and CEA (Gordon and McBride 1994,



In a three-dimensional state space, the planar platform of this diagram presented by Fig. 1.12 is at the level of the initial pressure,  $p_i$ . For higher pressures, the e-w platform is at higher levels. For the regime of pressures and temperatures existing in internal combustion engines, the reactants are made out of fixed fuel and air fractions, while, according to the available source of thermodynamic data, these components are perfect gases. The locus of states of the reactants,  $R$  is, therefore, pressure independent. However, the locus of states of the products,  $P$ , is dependent on pressure, because, in order to comply with the condition of thermodynamic equilibrium, their composition is variable. On the e-w plane, for higher pressures, the line of  $P$  tends to get straighter, so that, as indicated in Fig. 1.12, it is further away from the internal energy axis.

In the course of an exothermic process, the states of reactants,  $R$ , and products,  $P$ , move along their loci of states, starting from the initial point,  $\mathbf{i}$ , and ending at the terminal point  $\mathbf{t}$ , where the generation of products, and hence, consumption of fuel, is terminated, that, in principle, is different than the final point,  $\mathbf{f}$ . Nonetheless, as demonstrated in Chapter 3, they are coincident. The change of state taking place in the course of exothermic reaction, when the reactants are transformed into products at a fixed pressure, is presented by a straight line between a point on  $R$  and a point on  $P$ .

The changes of state of the reactants,  $R$ , and products,  $P$ , taking place in the combustion system are presented for them by vectors  $\mathbf{i} - \mathbf{t}$  along their loci of states, while the processes of exothermic reactions carrying out the transition between them are depicted by vectors  $\mathbf{i}_{\text{on } R} - \mathbf{i}_{\text{on } P}$  and  $\mathbf{t}_{\text{on } R} - \mathbf{t}_{\text{on } P}$  across their loci of states.

## 1.3.2 Processes

### 1.3.2.1 Mixing

For a chemical reaction to take place, its components must be first mixed to form a molecular aggregate. If, initially, the thermodynamic coordinates of fuel and air are different, they have to be brought to the same state  $\mathbf{i}$  on  $R$  - a task accomplished physically by transport processes of molecular mass diffusion and thermodynamic conduction, assisted by viscosity. In Fig. 1.12, the concomitant changes of state taking place in the course of mixing are expressed by broken curves between points  $\mathbf{o}$  on  $A$  and  $\mathbf{o}$  on  $F$  to point  $\mathbf{i}$  on  $R$ , with their directions indicated by arrows. The effect of mixing is manifested by rotation of the end point of the state vector around point  $\mathbf{i}$  on  $R$ . Irrespectively of the influence of molecular diffusion, which,



as a rule, must be involved in forming the reacting mixture, its outcome can be identified right from the outset by the intersection of the straight line between points **o** on A and **o** on F with R.

### 1.3.2.2 Exothermic Reaction

Chemical reaction of combustion takes place in an exothermic center. The concept of exothermic centers has been known for a long time in detonation literature under the name of “hot spots.” Their non-steady behavior under the influence of molecular diffusion has been studied extensively as the process of ignition (e.g. Boddington et al 1971; Gray and Scott 1990; Griffiths 1990). Their non-steady version in a turbulent field is referred to as the ‘flamelet model’ (Peters 2000). The fluid dynamic features of exothermic centers were investigated experimentally and theoretically in connection with their relevance to detonation and explosion phenomena, leading to the identification of mild and strong ignition centers. In a gasdynamic field where exothermic reaction takes place, exothermic centers occur at discrete sites. Each of them behaves then as a point singularity - a constant pressure deflagration where a finite change of state takes place locally at constant pressure - rather than across a straight line as it does in the classical version of a deflagration front.

### 1.3.3 Thermodynamic Parameters

The behavior of a combustion system is specified by the balances of mass, volume and internal energy. The mass balance is expressed simply by the fact that  $Y_S = \sum y_K = 1$ , or  $X_F = \sum x_K = Y_R$ , as depicted in Fig. 1.1.

The balance of volumes,  $v_S = \sum y_K v_K$  is expressed by the balance of dynamic potential,  $w_S = \sum y_K w_K$ , since by definition  $w(t) = p(t)v(t)$ , where  $p(t)$  is the same for all the components. The balance of energy is similarly given by  $e_S = \sum y_K e_K$ .

The two coordinates of the thermodynamic states are expressed by a single generalized state parameter,  $z_K = w_K, e_K$  ( $K = S, F, A, P, B, C, R$ ), in terms of which the balances of volume and energy are cast into a single equation,

$$z_S = y_F z_F + y_A z_A + y_P z_P + y_B z_B \quad (1.10)$$

whence, in view of (1.3) and (1.4),

$$z_S = Y_F z_F + Y_A z_A + Y_B z_B + (Y_P z_P - Y_F z_F - Y_A z_A) x_F \quad (1.11)$$

The state of the cylinder charge, C - a substance whose composition is fixed by initial conditions while its thermodynamic parameters vary,

$$z_C \equiv Y_F z_F + Y_A z_A + Y_B z_B \quad (1.12)$$

The state of reactants, R, considered as a mixture of fuel, F, with air, A, at their fixed ratio of  $\sigma_R$  is determined by the mass average

$$z_R = \frac{Y_F z_F + Y_A z_A}{Y_F + Y_A} = \frac{z_F + \sigma_R z_A}{1 + \sigma_R} \quad (1.13)$$

With (1.12) and (1.13), in view of (1.8), (1.13) is reduced to

$$z_S - z_C = (z_P - z_R) y_P \quad (1.14)$$

In a combustion field, an exothermic center is a front across which a jump from **i** to **t** takes place at a constant pressure. Its amplitude is

$$z_{SP} - z_{SR} = Y_R (z_P - z_R) \quad (1.15)$$

Presented in Fig. 1.13 are changes of state taking place in the general case of an exothermic system that, unlike that of Fig. 1.12, is affected by energy losses occurring in the course of the transition from R to P. Under such circumstances, the end equilibrium states on P are, below those reached at constant enthalpy.

### 1.3.4 Coordinate transformation

$$C_K \equiv (e_t - e_i)_K / (w_t - w_i)_K \quad (K = R, P) \quad (1.16)$$
$$e_R = C_R w_R \quad (1.17)$$
$$e_P = C_P w_P - q_P \quad (1.18)$$

where  $q_p = e_{R0} - e_{P0}$ , subscript “o” referring to the intersections of the lines of K with the axis of ordinates. The quantity  $q_p$ , referred to here as the exothermic energy, provides a geometric measure of a reference parameter that replaces the conventional concept of ‘heat release’ (HR), used as a constant in conjunction with fixed specific heats. Its awkward role when specific heats are variable is evident in Fig. 1.13, where the reference states of HR are denoted by r.

According to (1.17) and (1.18),

$$e_R - e_P = C_R w_R - C_P w_P + q_P \quad (1.19)$$

The coordinates of internal energy,  $e_K(w_K)$ , can be thereby expressed in terms of the local trajectory slope,  $C_K$ , and the exothermic energy,  $q_P$ , as illustrated in Fig. 1.14 for the initial state, **i**, and the terminal state, **t**, of transition from a reactant, R, to product, P, taking place in an adiabatic exothermic center.

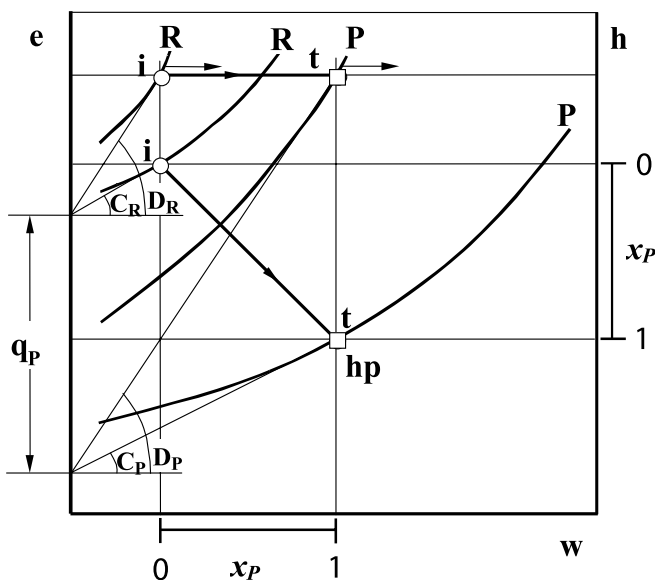


**Fig. 1.14.** Diagram of states for an adiabatic exothermic center in  $e(w)$  and  $h(w)$  coordinates

The loci of states for R and P are displayed in this figure in  $e(w)$  and  $h(w)$  coordinates. A change of state taking place in the course of an adiabatic exothermic reaction proceeds along a constant enthalpy path – a diagonal on the plane of  $e-w$  expressed by  $e = h_i - w$ , and a horizontal line on the  $h-w$  plane. As implied by the geometry of this diagram, the slope  $D_K = C_K + 1$  ( $K = R, P$ ). If the reactants are considered as perfect gases with constant specific heats,  $(c_v)_K = de_K/dT$  and  $(c_p)_K = dh_K/dT$ , then, in terms of  $R_K \equiv R/M_K$ , where  $R$  is the gas constant and  $M_K$  the molar mass, whence  $\gamma_K \equiv c_{Kp}/c_{Kv}$ ,  $C_K = c_{Kv}/R_K = 1/(\gamma - 1)$  and  $D_K = c_{Kp}/R_K = \gamma/(\gamma - 1)$ .

Since, generally, the curvature of a state trajectory, R or P, is relatively small, the changes of state performed by reactants and products in the course of an exothermic process are expressed with remarkable accuracy by straight lines. The relationships for trajectory slopes specified in the previous section can be applied, therefore, to the sectors pertaining to the process of an exothermic center.

### 1.3.5 Isentropic Relationships

Of particular significance to the coordinates of the state diagram are the isentropic relationships. Irrespectively whether the substance is a perfect gas or not, nor whether its process is isentropic or not, the parameter

$$\Gamma \equiv \left(\frac{\partial h}{\partial e}\right)_p = 1 + \left(\frac{\partial w}{\partial e}\right)_p = \frac{C_k + 1}{C_k} = \frac{D_k}{D_k - 1} \quad (1.20)$$

while the polytropic index

$$n \equiv \frac{d \ln p}{d \ln \rho} = - \frac{\nu}{p} \frac{dp}{d\nu} \quad (1.21)$$

Then, by virtue of the Second Law, according to which

$$\begin{aligned} Tds &= de + pdv \\ &= dh - \nu dp \end{aligned} \quad (1.22)$$

the isentropic index, with subscript “s” denoting an isentropic process,

$$\gamma \equiv n_s = \left(\frac{\partial h}{\partial e}\right)_s = - \frac{\nu}{p} \left(\frac{\partial p}{\partial \nu}\right)_s = \Gamma_s \quad (1.23)$$

Thus, noting that  $\frac{p}{\rho} \equiv pv \equiv w$ , the velocity of sound

$$a \equiv \sqrt{\left(\frac{\partial p}{\partial \rho}\right)_s} = \sqrt{\gamma \frac{p}{\rho}} = \sqrt{\gamma w} \quad (1.24)$$

whence

$$\left(\frac{\partial a}{\partial p}\right)_s = \frac{\gamma}{2a} \left[\frac{\partial (w)}{\partial p}\right]_s \quad (1.25)$$

while, in view of (1.21) and (1.23),

$$\left[\frac{\partial (w)}{\partial p}\right]_s = v + p \left(\frac{\partial v}{\partial p}\right)_s = v \left(1 - \frac{1}{\gamma}\right) = \frac{\gamma - 1}{\gamma} v \quad (1.26)$$

so that, by virtue of (1.24),

$$\left(\frac{\partial p}{\partial a}\right)_s = \frac{2}{\gamma - 1} \rho a = \frac{2\gamma}{\gamma - 1} \frac{p}{a} \quad (1.27)$$

- a relationship of particular significance to gasdynamics presented in Chapter 7.

Since, by definition,  $dw = w(d\ln p + d\ln v)$ , it follows from (1.26) that

$$dw = \frac{\gamma - 1}{\gamma} w d\ln p \quad (1.28)$$

and, according to (1.20),

$$de \equiv C_k dw = \frac{1}{\gamma - 1} dw = \frac{p}{\gamma \rho} d\ln p \quad (1.29)$$

- a relationship of particular significance to blast wave theory presented in Chapter 9.

### 1.3.6 Closed System

A closed system is one whose volume,  $v(t)$ , is restricted by prescribed boundary conditions. In the cylinder of an internal combustion engine, for instance, the boundary conditions are imposed by piston motion estab-

lished by the kinematics of crankshaft mechanism. Its volume and energy balances are specified by (1.14), for which  $w_S(t)$  is prescribed.

The volume balance is then obtained for  $z = w$ , while  $p_R = p_P$ , so that

$$(w_P - w_R) y_P = w_S - w_C \quad (1.30)$$

The energy balance is obtained similarly for  $z = e$ , whence

$$(e_P - e_R) y_P = e_S - e_C \quad (1.31)$$

for which

$$e_S = e_{Si} - e_e \quad (1.32)$$

while

$$e_e \equiv w_w + q_w \quad (1.33)$$

expresses the energy expenditure that, in an internal combustion engine, consists of piston work,

$$w_w \equiv v_c \int_i^t (p - p_b) dv_s \quad (1.34)$$

and the energy loss,  $q_w$ .

In the above, subscript “c” denotes clearance volume per unit mass, while “b” refers to the backpressure, whereas  $q_w$ , is incurred primarily by heat transfer to the walls that, besides some usually negligible effects of leakage and mixing, is the principal irreversibility of a combustion system.

With (1.19) and (1.32), the energy balance specified by (1.31) becomes

$$(C_R w_R - C_P w_P + q_P) y_P = C_C (w_C - w_{Si}) + e_e \quad (1.35)$$

Then, eliminating  $w_P$  from (1.30) and (1.35), the mass fraction of products

$$y_P = \frac{C_P (w_S - w_C) + C_C (w_C - w_{Si}) + e_e}{q_P + C_R w_R - C_P w_R} \quad (1.36)$$

In terms of normalized variables,  $W_K \equiv w_K / w_{Si}$  ( $K = S, R, P$ ) and  $W_e \equiv e_e / w_{Si}$ , while  $Q_P \equiv q_P / w_{Si}$ , (1.36) yields

$$y_P = \frac{C_P(W_S - 1) - (C_P - C_C)(W_C - 1) + W_e}{Q_P - (C_P - C_R)W_R} \quad (1.37)$$

Since, according to JANAF tables – the conventional sources of thermodynamic data – all the components are treated as perfect gases, while the thermodynamic properties of the reactants and the system charge – their mixtures at fixed composition – are practically the same,

$$W_C = W_R = P^m \quad (1.38)$$

where  $m \equiv 1 - n_c^{-1}$ .

Thus, according to the volume balance expressed by (1.30),

$$W_P = W_R + \frac{W_S - W_C}{y_P} = P^m + \frac{PV - P^m}{y_P} \quad (1.39)$$

- a relationship emphasising the singular nature of state **i**, at which the numerator  $W_S - W_C = 0$ , while the denominator  $y_P = 0$ .

According to the results of a comprehensive, semi-empirical study of heat transfer in a closed combustion vessel presented in Chapter 3, the mass fraction of products,  $y_P(\Theta)$  is equivalent to  $x(\tau)$ , the latter identified by (2.49) with (2.48).

The mass fraction of the generated products, as pointed out in (1.15),

$$y_P = y_E + y_I \quad (1.40)$$

where  $y_E$  is its effective part and  $y_I$  is the ineffective part. Then, by virtue of (1.37) and (1.38), with  $W_w \equiv w_w / w_{Si}$ , while, by definition,  $W_S = PV$  where  $P \equiv p / p_i$ ,  $V \equiv v_S / v_{Si}$ ,

$$y_E = \frac{C_P(PV - 1) - (C_P - C_C)(P^m - 1) + W_w}{Q_P - (C_P - C_R)P^m} \quad (1.41)$$

while, in turn, the effective part,  $y_E$ , consists of the products generated for internal energy,  $y_\epsilon$ , and to produce piston work,  $y_\omega$ , so that



$$y_E = y_\varepsilon + y_\omega \quad (1.42)$$

where

$$y_\varepsilon = \frac{C_P(PV - 1) - (C_P - C_C)(P^m - 1)}{Q_P - (C_P - C_R)P^m} \quad (1.43)$$

and

$$y_\omega = \frac{W_w}{Q_P - (C_P - C_R)P^m} \quad (1.44)$$

while the ineffective part

$$y_I = \frac{Q_I}{Q_P - (C_P - C_R)P^m} \quad (1.45)$$

where  $Q_I \equiv q_w / w_{Si}$ .

It is of interest to note that, if  $C_P = C_C = C_R$ , (1.41) is reduced to

$$y_E = \frac{(PV - 1) + W_w}{Y_R Q_P / C_P}$$

- a relationship of the well established "heat release analysis", based on the classical paper of Rassweiler and Withrow (1938).

For an isochoric and isentropic system of  $v = 1$ ,  $W_w = 0$  and  $Q_I = 0$ , obtained thereby is the popular proportionality between the mass fraction of products,  $y_P$ , and the measured overpressure,  $(P - 1)$  [vid. e.g. the classical text of Lewis and von Elbe (1987)].

The procedure of pressure diagnostics is completed by taking into account the results obtained from heat transfer study described in Chapter 3. According to them,

- (1) the time coordinate of the final state is identified with that of the terminal state, so that  $\Theta_f = \Theta_t$
- (2) the mass fraction of products is identified with the progress variable for the polytropic function expressed in terms of the life function, while  $y_P(\Theta) = x(\Theta)$ , determined for the exothermic process, whose profile is displayed by Fig. 1.8.

Obtained therefore are means for evaluating the ineffective mass fraction of products  $y_I = y_P - y_E$ , identifiable, as demonstrated in Chapter 3, with energy loss incurred by heat transfer to the walls. The relationship between these variables is displayed on the phase diagram illustrated by Fig. 1.15, corresponding to their profiles displayed by Fig. 1.2.

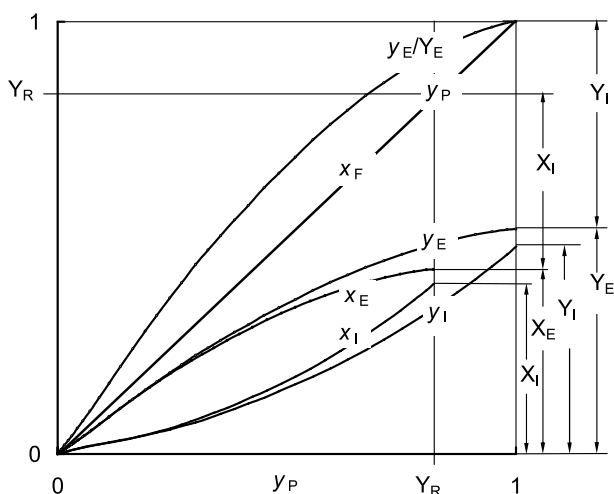


**Fig. 1.15.** Phase diagram of the effective and ineffective parts of products

Concomitantly, (1.39) yields the profiles of the dynamic potential and, hence, the temperature profiles of the reactants and the products. The results obtained thereby from dynamometer tests of a diesel engine were found to be in satisfactory agreement with the well-known Woschni correlation [Woschni 1966/67, 1967, 1970, Woschni and Anisits 1973, 1974].

### 1.3.7 Procedure

As for the elucidation of dynamic properties, the procedure for implementation of the exothermic process is presented here for the specific example of a HCCI engine.

The state diagram of its exothermic process is presented by Fig. 1.16. Its parameters are presented by Table 1.5. Profiles of the mass fraction of products,  $y_P = x$ , its effective part,  $y_E$ , consisting of  $y_e$  and  $y_o$ , are determined with the use of these parameters, according to (1.40), by (1.41), that, according to (1.42), by (1.43) and (1.44). The results are displayed by Fig. 1.17. The dynamic potential in its normalized form,  $W_K$ , is thereupon

obtained by virtue of (1.39), and its profile,  $w_K(\Theta) = W_K(\Theta)w_{Si}$ , where  $K = R, P, S$ , is presented by Fig. 1.18, whence the temperature profiles depicted by Fig. 1.19, are evaluated the use of the equation of state whence  $T_K(t) = w_K/R_K$ .

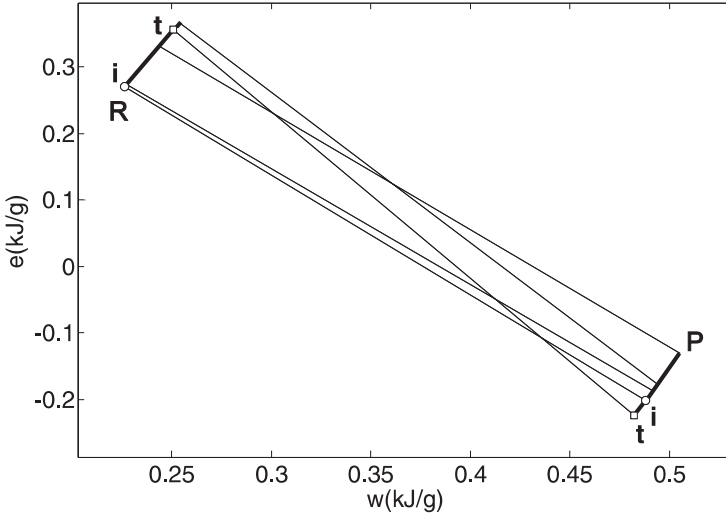


**Fig. 1.16.** State diagram of the exothermic process in the HCCI engine

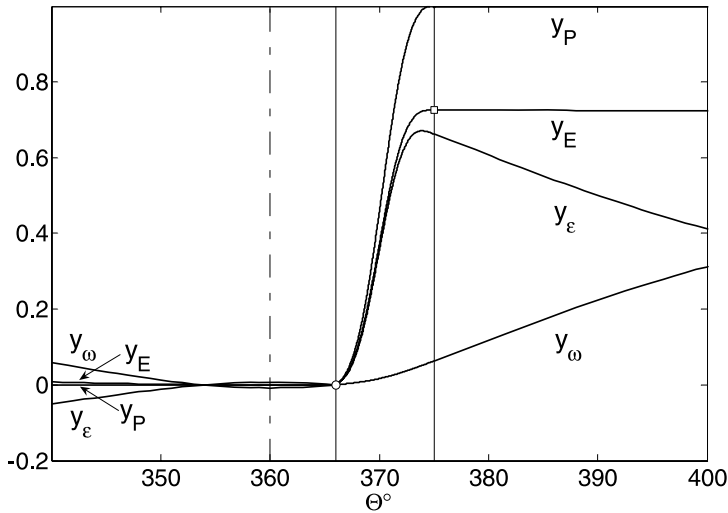


**Fig. 1.17.** Profiles of the mass fraction of products and its components of the HCCI engine

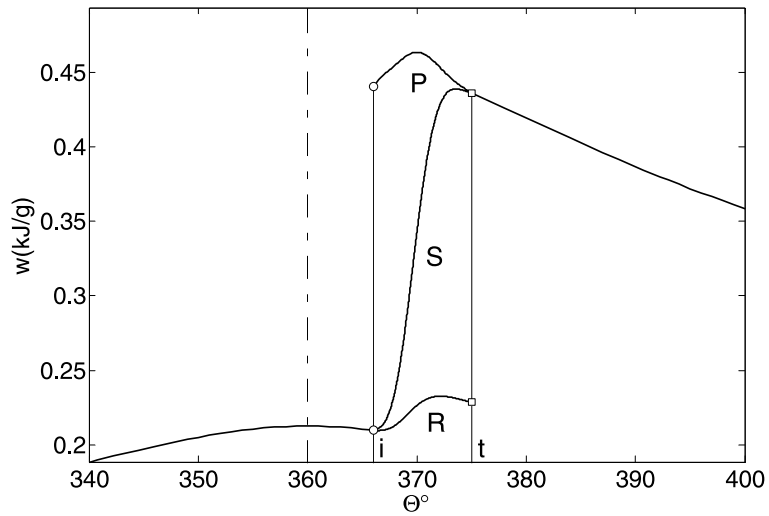


**Fig. 18.** Profiles of the dynamic potential of the HCCI engine

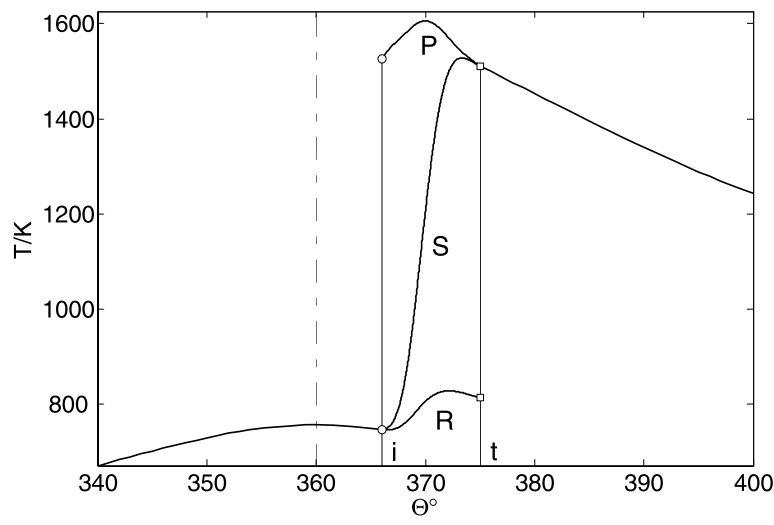


**Fig. 1.19.** Temperature profiles in the HCCI engine

### 1.3.8 Control Logistics

Pressure diagnostics provides the analytical method for ushering in micro-electronic control system to optimize the execution of the exothermic process of combustion and improve thus significantly its performance. Put forth thereby is the essential objective of what is referred to as ‘internal treatment’ – a technology that has been aborted by industry in favor of ‘external treatment’ as a consequence of the fact that, at the time when clean air laws were introduced, micro-electronics was not yet available.

The benefits of internal treatment are realized by implementing the principles of Aero-thermo-chemistry introduced by von Karman: *fluid dynamics* to create turbulent plumes as far away from the walls as possible, *thermodynamics* to reveal their physical properties and assess their effectiveness, and *chemistry* to modulate the chemical kinetic process of the exothermic reaction of combustion so that it takes place at the lowest temperature allowable at the verge of extinction.

In effect, one is treating, therefore, an inverse problem of the inverse problem of pressure diagnostics: upon assessing the performance of a combustion system on the basis of the measured pressure profile, its execution is optimized by controlling its operating conditions. A closed-loop micro-electronic control system suitable for this purpose is described in Oppenheim 2004. Its primary feedback is a pressure transducer; its principal actuators are provided by a pulsed jet injector and a pulsed flame jet igniter.

Presented here for illustration is the simplest example of optimization attainable by micro-electronic control, one particularly appropriate for HCCI engines: shifting of the exothermic process of combustion so that it takes place as close as possible to the top dead center – a task akin to engine tuning for maximum torque.

The logistics of control are implemented in two steps:

- (1) shift of the exothermic process to the top dead center
- (2) reduction of the thus augmented IMEP of the work cycle to its standard value

The application of this procedure is illustrated by the subsequent figures where the reference case is depicted by continuous lines, while the two steps are delineated, respectively, by broken and dotted lines, and in the labels they are marked by single and double primes.

As depicted in Fig. 1.20, the profile of the polytropic function is extended, first, by shifting the life function of the dynamic stage along the horizontal polytropes of the processes of compression and expansion, so that its point of inflection is at TDC (top dead center), and, thereupon, by decreasing the level of the expansion polytrope to provide the required work output.

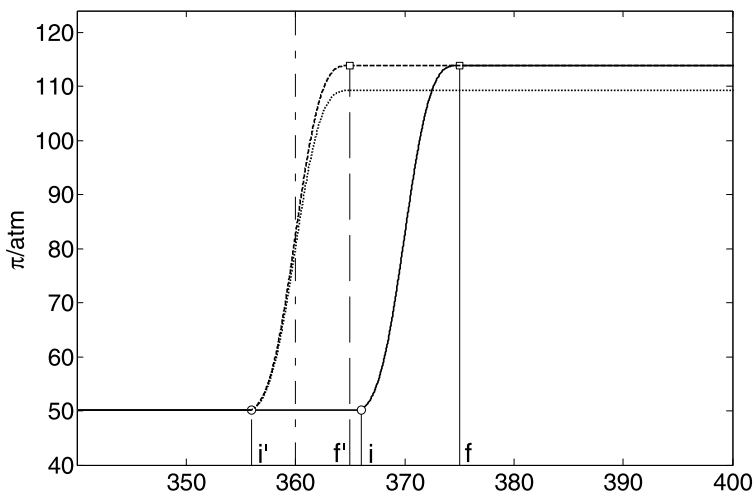


**Fig. 1.20.** Profiles of the polytropic functions for the HCCI engine in the original and controlled mode of operation

On this basis, all the parameters for the controlled mode of the engine combustion system are evaluated. The results are displayed by Figs. 1.21 – 1.26 in comparison to the original performance.

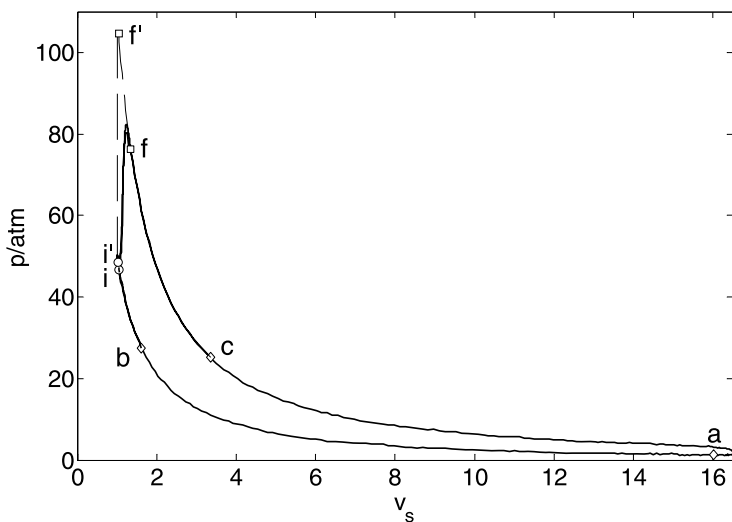


**Fig. 1.21.** Work cycle of the HCCI engine in the original and controlled mode of operation

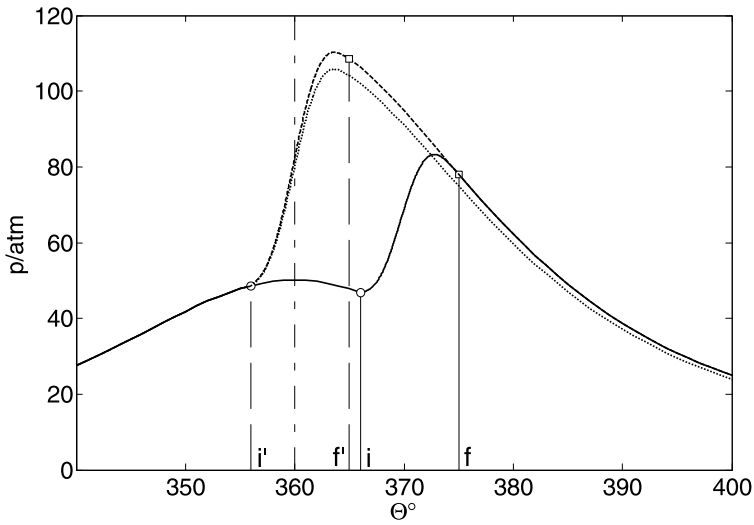


**Fig. 1.22.** Pressure profiles of the HCCI engine in the original and controlled mode of operation

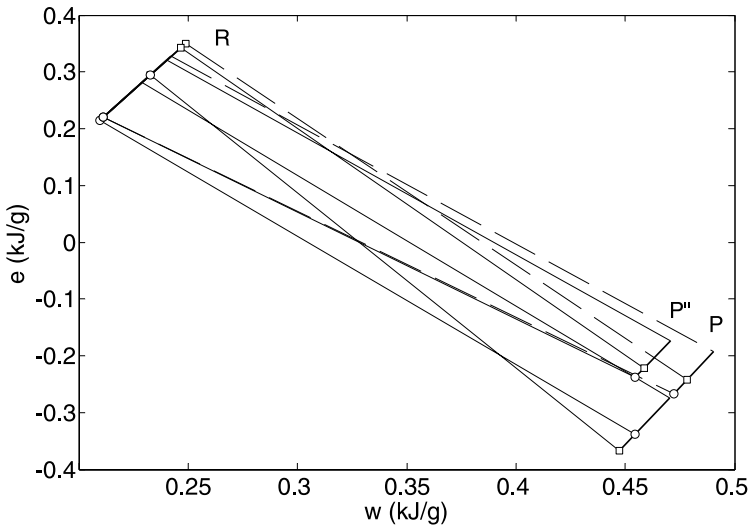


**Fig. 1.23.** State diagram of the HCCI engine in the original and controlled mode of operation

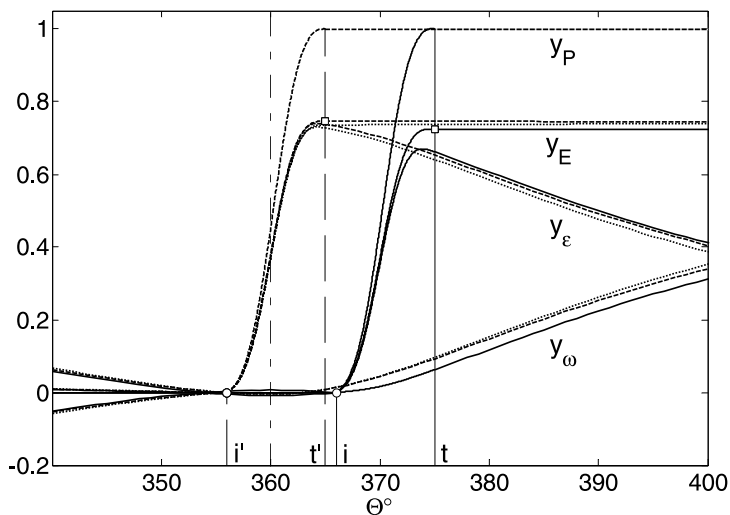


**Fig. 1.24.** Profiles of the mass fraction of products and its components of the HCCI engine in the original and controlled mode of operation

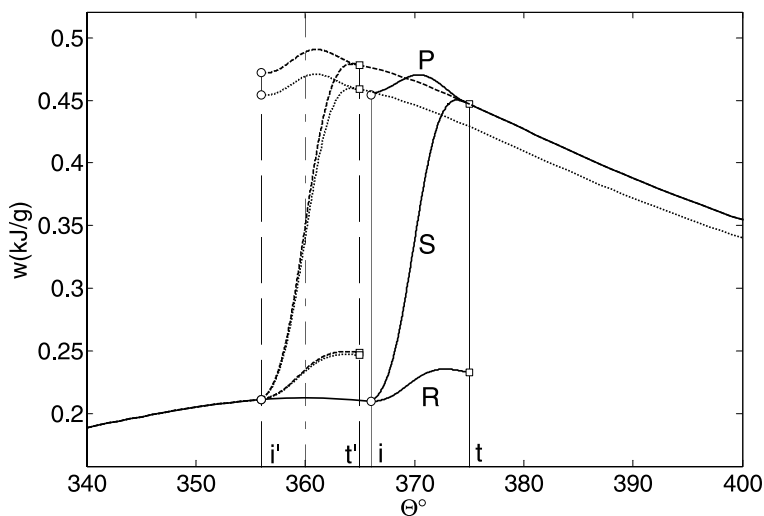


**Fig. 1.25.** Profiles of dynamic potential for the HCCI engine in the original and controlled mode of operation



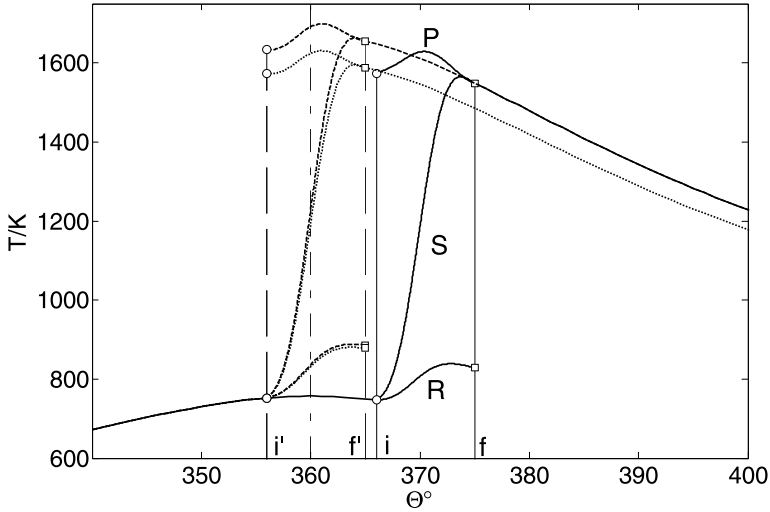


**Fig. 1.26.** Temperature profiles of the HCCI engine in the original and controlled mode of operation

Since the work cycle of the HCCI engine is kept invariant in the original and controlled mode of operation, it follows from (1.2) for  $K = R$  that, with the same exothermic energy per unit mass (referred to popularly as calorific or “heating” value) and the same mass fraction of reactants,

$$\frac{\text{IMEP}''}{\text{IMEP}'} = \frac{Y_F''}{Y_F'} = \frac{1 + \sigma_{st} \lambda}{1 + \sigma_{st} \lambda''} \quad (1.46)$$

whence

$$\lambda'' = [(1 + \sigma_{st} \lambda) \frac{\text{IMEP}'}{\text{IMEP}''} - 1] / \sigma_{st} \quad (1.47)$$

yielding

$$\frac{Y_F''}{Y_F'} = \frac{1 + \sigma_{st} \lambda}{1 + \sigma_{st} \lambda''} \frac{Y_E}{Y_E''} \quad (1.48)$$

Provided thus is an expression for the mass fraction of fuel in the controlled and uncontrolled cases. The results based on the data of Figs. (1.21) and (1.24), are presented by Table 1.5.

**Table 1.5.** Parameters of thermodynamic properties

Step	0	1	2
$\Theta_i$	366		3.56
$\Theta_f$	375		365
IMEP/atm	7.77	8.36	7.77
$\lambda$	2.2		2.37
$C_R$	3.4839		3.4839
$C_P$	4.0145		3.9448
$Q_P$	7.3649		6.7781
$Y_E$	0.7247	0.7465	0.7361

According to the above, the ratio of mass fractions of fuel expended in

$$\frac{Y_F''}{Y_F} = \frac{(1 + 12.305 \cdot 2.2) \cdot 0.7247}{(1 + 12.305 \cdot 2.37) \cdot 0.7361} = \frac{20.3431}{22.2029} = 0.916$$

The saving in fuel consumption obtained by controlled operation of the engine is therefore 8.4% – a gain associated with equivalent reduction in the formation of pollutants. This type of improvement can be advanced significantly further by charge stratification, so that, within the relatively short lifetime of the dynamic stage, the combustion zone is kept away from the walls, whereby the energy loss incurred by heat transfer to the surroundings is diminished, as demonstrated in Chapter 4.

## 1.4 Production Engine

To illustrate the application of pressure diagnostics to an industrial product, consider a Renault spark ignition engine operating at full and part loads, the latter being most often encountered in the European driving cycle [Gavillet et al. 1993; Oppenheim et al 1997, Oppenheim 2004]. Its specification is provided by Table 1.6.

**Table 1.6.** Engine Data

Model	F7P-700
Bore(mm) x stroke(mm)	82.0 x 83.5
Cylinders	4
Piston rod length (mm)	144
Compression ratio	10

### 1.4.1 Full Load

The operating conditions of the dynamometer test at full load are specified by Table 1.7.

**Table 1.7.** Operating conditions of the Renault engine operating at full load

Speed (rpm)	2000
Torque (Nm)	128
BMEP (kPa)	912
Fuel	RON 95
Fuel flow (gm/min)	32
$\lambda$	1
$\sigma$	15.0
$P_i/\text{atm}$	1
$T_i/\text{K}$	300
$n$	1.323

#### 1.4.1.1 Dynamic Properties

Parameters of the dynamic properties and the life function are presented by Table 1.8.

**Table 1.8.** Parameters of dynamic properties and the life function for Renault engine operating at full load

$\theta_i$	353
$\theta_f$	384
$\alpha_\pi$	9.38
$\chi_\pi$	1.29

The characteristic features of the dynamic properties are displayed by Figs. 1.27-1.30 in terms of, respectively, the measured pressure profile,  $p(\Theta)$ , the work cycle in linear scales,  $p(v)$ , the profile of the polytropic function,  $\pi(\Theta)$ , and the progress parameter of fuel consumption in the course of the dynamic stage,  $x_\pi(\Theta)$ , together with the analytic expression for the pressure profile based on the life function.

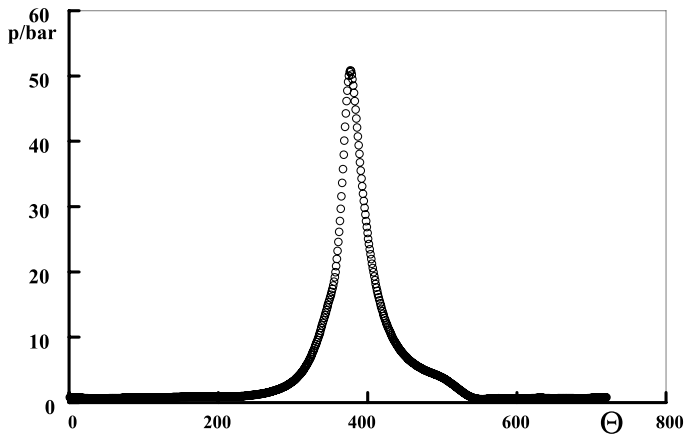


Fig. 1.27. Measured pressure profile of the Renault engine operating at full load

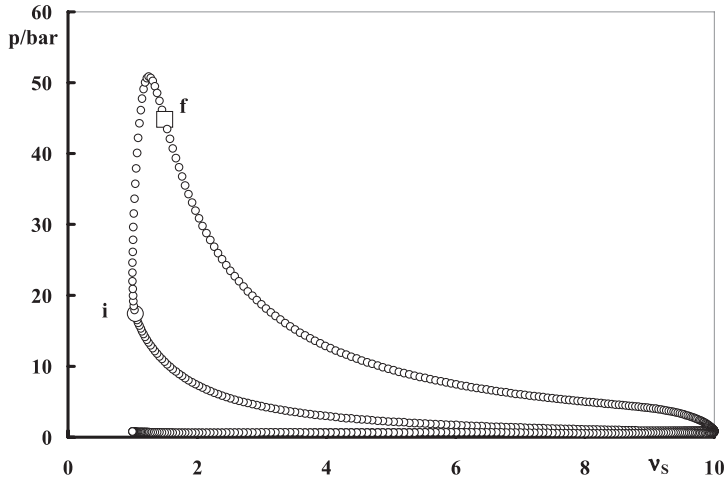
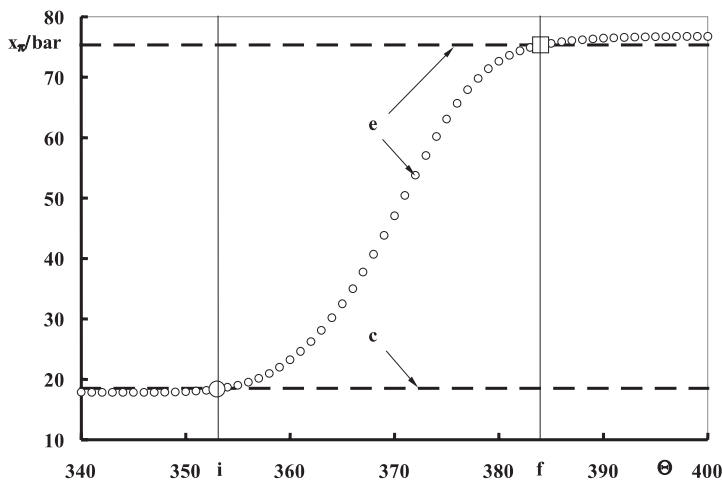
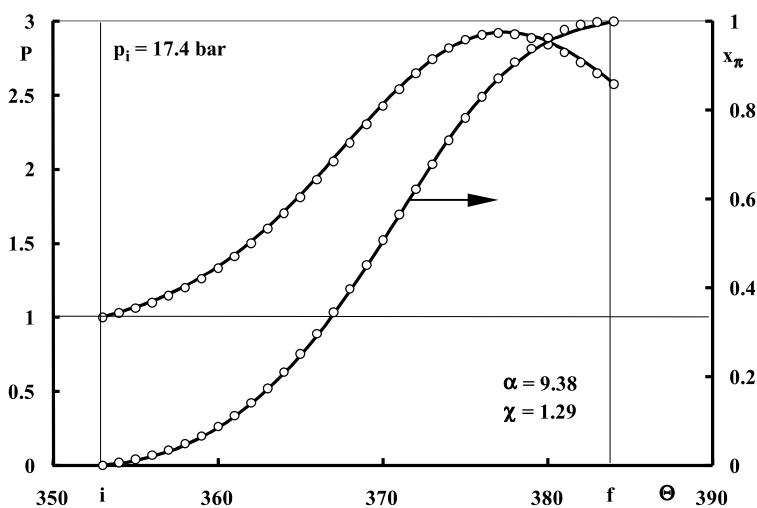


Fig. 1.28. Work cycle in linear scales of the Renault engine operating at full load



**Fig. 1.29.** Profile of polytropic functions for the Renault engine operating at full load



**Fig. 1.30.** Profiles of the measured pressure data in normalized form,  $P(\Theta) \equiv p/p_i$ , and the progress parameter of consumed fuel,  $x_\pi(\Theta)$ , (presented by circles) and the polytropic function expressed in terms of the life function (displayed by continuous lines) for the dynamic stage in the Renault engine operating at full load

### 1.4.1.2 Thermodynamic Properties

The thermodynamic parameters of the working substance are presented by Table 1.9.

**Table 1.9.** Thermodynamic parameters of Renault engine operating at full load

		p	T	v	u	h	w	M
	States	atm	K	m <sup>3</sup> /g		kJ/g		g/mol
F	i	17.18	623	26.206	1.2294	-1.1838	0.0456	113.53
	f	44.24	637	10.412	1.1868	-1.1401	0.0467	
R	i	17.18	623	98.328	0.0693	0.24046	0.1712	30.258
	f	44.24	772	47.295	0.2092	0.42124	0.2120	
	uv	141.65	2870	98.328	0.0693	0.9176	0.8483	28.131
P	hp	17.18	2515	423.87	0.4975	0.2405	0.7380	28.330
	pT	17.18	623	104.01	2.7255	-2.5444	0.1811	28.606

The coordinates of the thermodynamic states of the components are listed in Table 1.10.

**Table 1.10.** State parameters of Renault engine operating at full load

K	C <sub>K</sub>	u <sub>K0</sub>	q <sub>K</sub>
A	2.7673	-0.3412	0
F	38.7273	-2.995	2.654
R	3.4281	-0.5176	0.1764
P	5.1373	-4.2886	3.9474

The state diagram of the exothermic process in the course of the dynamic stage is displayed by Fig. 1.31.

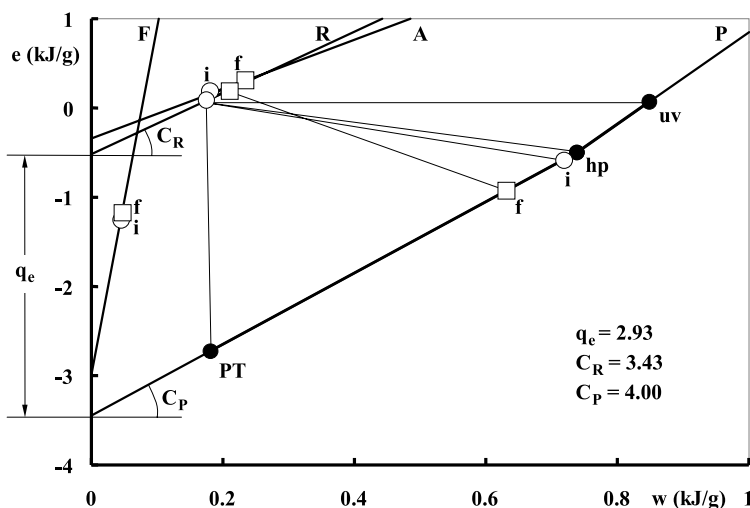


**Fig. 1.31.** State diagram of the exothermic process in the course of the dynamic stage for the Renault engine operating at full load

Profiles of the normalized temperatures,  $\tilde{T}_K \equiv T_K / T_i$ , and specific volumes,  $\tilde{v}_K \equiv v_K / v_i$ , are depicted by Fig. 1.32.

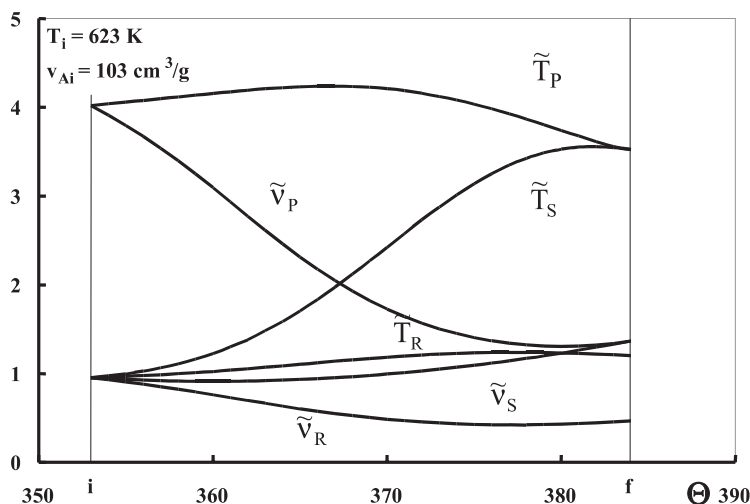


**Fig. 1.32.** Profiles of normalized temperatures and specific volumes in the course of the dynamic stage in the Renault engine operating at full load

1.4.2 Part load

The operating conditions and life function parameters of the Renault engine run at part load are as follows.

1.4.2.1 Dynamic Properties

**Table 1.11.** Operating conditions and life function parameters of Renault engine run at part load

Speed (rpm)	2000
Torque (Nm)	9.83
BMEP (kPa)	70
Fuel	RON 95
Fuel flow (gm/min)	32
$\lambda$	1
$\sigma$	15.0
$P_i$ /atm	0.6
$T_i$ /K	300
$n$	1.365
$x_\pi$	$\alpha$ 14.2
	$\chi$ 2.78

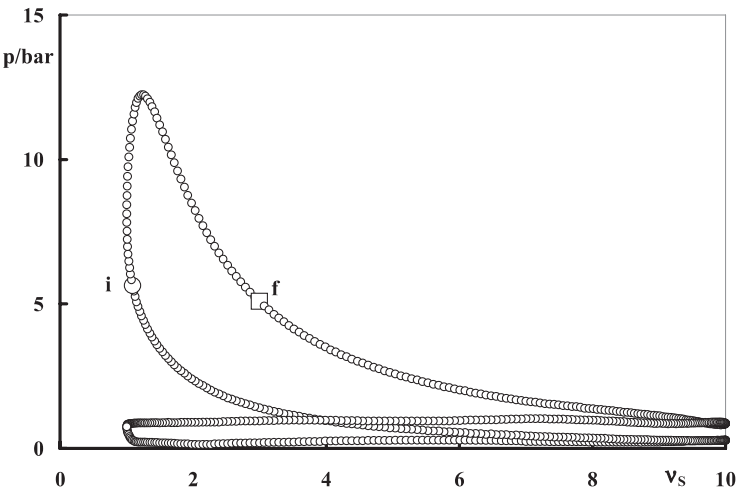


**Fig. 1.33.** Work cycle of the Renault Engine operating at part load

The work cycle of the Renault engine operating at part load is presented by Fig. 1.33. The profile of the polytropic function for the dynamic stage



is displayed in Fig. 1.34, while profiles of the progress parameter  $x_\pi(\Theta)$  and of the normalized pressure,  $P(\Theta) \equiv p(\Theta)/p_i$ , represented by its measured data (marked by circles) and its analytic expressions (delineated by continuous lines), is depicted in Fig. 1.35.

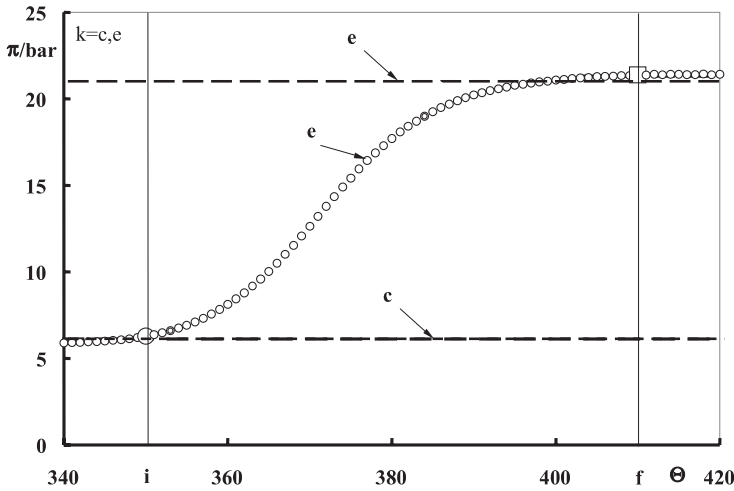


**Fig. 1.34.** Profile of the polytropic function for the dynamic stage in the Renault engine operating at part load

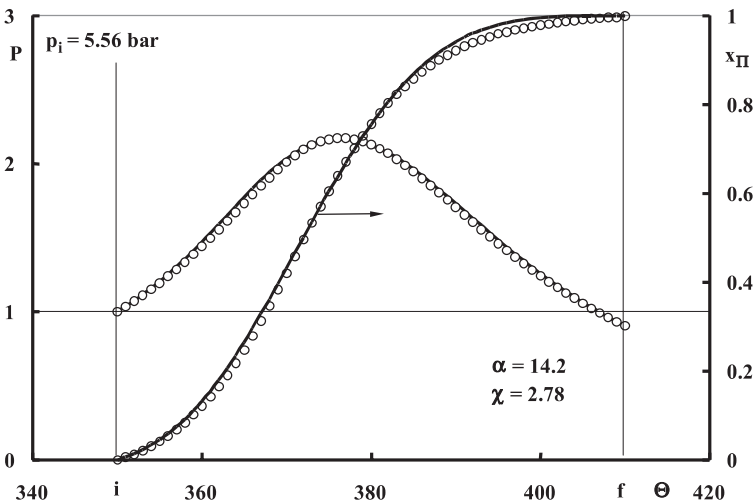


**Fig. 1.35.** Profiles of the measured pressure data in normalized form,  $P(\Theta) \equiv p / p_i$ , and the polytropic function of the dynamic stage for the Renault engine operating at part load

1.4.2.2 Thermodynamic Properties

The thermodynamic state parameters of the exothermic process in the Renault engine operating at part load are specified in Table 1.12.

**Table 1.12.** State parameters of the dynamic properties of the Renault engine operating at part load (Gavillet et al. 1993)

K	States	C	$u_o$ kJ/g
A	i	2.7857	0.3459
	f		
F	i	54.0000	3.7857
	f		
R	i	3.0192	0.4364
	f		
P	uv	5.4725	4.4670
	hp	4.2093	3.5230
	PT		

Profiles of the normalized temperature,  $\tilde{T}_K \equiv T_K / T_i$ , and specific volume,  $\tilde{v}_K \equiv v_K / v_i$ , are depicted in Fig. 1.36.

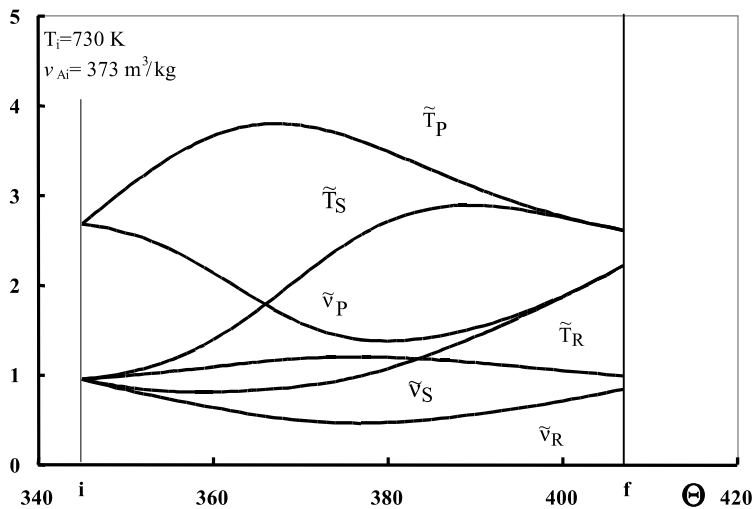


**Fig. 1.36.** Profiles of normalized temperatures and specific volumes in the course of the dynamic stage for the Renault engine operated at part load



<http://www.springer.com/978-3-540-77363-4>

Dynamics of Combustion Systems

Oppenheim, A.K.

2008, XXI, 368 p., Hardcover

ISBN: 978-3-540-77363-4